Journal Pre-proofs

Short Communications

Ultra-high conductive graphene assembled film for millimeter wave electromagnetic protection

Rongguo Song, Shaoqiu Jiang, Zelong Hu, Chi Fan, Peng Li, Qi Ge, Boyang Mao, Daping He

PII: S2095-9273(22)00111-6
DOI: https://doi.org/10.1016/j.scib.2022.03.014
Reference: SCIB 1725

To appear in: *Science Bulletin*

Received Date: 14 November 2021
Revised Date: 28 January 2022
Accepted Date: 15 March 2022

Please cite this article as: R. Song, S. Jiang, Z. Hu, C. Fan, P. Li, Q. Ge, B. Mao, D. He, Ultra-high conductive graphene assembled film for millimeter wave electromagnetic protection, *Science Bulletin* (2022), doi: https://doi.org/10.1016/j.scib.2022.03.014

Short Communication

Received 14 November 2021
Received in revised form 28 January 2022
Accepted 15 March 2022

Ultra-high conductive graphene assembled film for millimeter wave electromagnetic protection

Rongguo Song[1], Shaoqiu Jiang[1], Zelong Hu[1], Chi Fan[2], Peng Li[1], Qi Ge[3], Boyang Mao[3]*, Daping He[1]*

1 Hubei Engineering Research Center of RF-Microwave Technology and Application, Wuhan University of Technology, Wuhan 430070, China

2 The National Key Laboratory of Antennas and Microwave Technology, Xidian University, Xi' an 710071, China

3 Chongqing 2D Materials Institute, Liangjiang New Area, Chongqing 400714, China

* Correspondence authors

Email addresses: maoboyang@gmail.com (B. Mao); hedaping@whut.edu.cn (D. He)

The millimeter wave frequency band is the main frequency band for 5G and future 6G applications that are becoming more mature. Millimeter wave devices can provide ultra-wide working bandwidth and ultra-fast transmission rates, allowing the implementation of many services such as smart city and smart home, Internet of Things (IoT), robot, and artificial intelligence (AI), all of which make our lives more convenient and intelligent [1]. With these advancements, the explosive growth of various electronic devices, especially mobile terminals, has created a serious problem of electromagnetic wave pollution, which not only harms human health but also disrupts the normal operation of electronic devices [2,3]. The tendency toward downsizing and multi-functioning of portable gadgets has exacerbated the problem of electromagnetic interference [4,5]. In addition to complete electromagnetic shielding, selective shielding of the electromagnetic field is important in many cases such as

WLAN, radome, and reflector antenna, to ensure the normal transmission of other frequency bands. As a member of metamaterials, frequency selective surface (FSS) is formed by periodic arrangement of structural units, which can selectively absorb, reflect and transmit electromagnetic waves (and act as a spatial filter) [6], thus is an effective way to realize frequency selection. Due to the excellent properties, FSSs have been widely used in base station antenna miniaturization, antenna beam control, decoupling and improving communication performance. The fabrication process of FSS is, however, complicated requiring multiple steps of lithography and etching. Thus, the effective and selective shielding of electromagnetic field via a facile approach is of great importance and becoming more urgent.

Materials with high conductivity are conventionally used to achieve good electromagnetic interference shielding effectiveness (EMI SE) including copper, iron, nickel, and other metal materials. However, with the rapid development of millimeter wave communication devices, high electrical conductivity is no longer the only practical standard for high electromagnetic shielding performance, while low cost, light weight, flexibility, low profile, scalable production, and corrosion resistance are also required (particularly in highly integrated and high frequency equipment). Recently, two-dimensional materials, such as MXene and graphene, have become the viable alternative materials in EMI shielding applications [7,8]. MXene has high electrical conductivity and can achieve good electromagnetic shielding performance at low thicknesses, but it can be easily oxidized (not suitable for long-term use) and difficult to fabricate in a large area, which hinder its practical application in real commercial shielding applications. Graphene, on the other hand, has good chemical stability and light weight. However, due to the poor electrical conductivity limited by conventional fabrication methods, its electromagnetic shielding effectiveness per unit thickness is relatively low (normally less than 2000 dB/mm) and thus difficult to satisfy the demand for low-profile EMI materials [9, 10]. For both MXene and graphene, complex structure shielding surface under millimeter wave communication band is not fully studied yet.

In this work, we improved the conductivity of graphene assembled film (GAF) by applying a secondary high temperature annealing and realized the large-scale production. Fig. 1a is the digital photo of large area GAF with the dimensional size about 0.5 m × 3 m. The detailed fabrication procedures of GAF are described in Experimental Section of Supplementary materials (online). GAF can be rolled up like

paper, proving that it can be mass-produced and has good self-supporting ability. The Mobius strip in Fig. 1a inert is an illustration that shows the high flexibility of GAF. After the secondary high temperature annealing, the conductivity of GAF tested by four probe methods [12] is 1.59×10^6 S/m, which is 41% higher than the single annealing treatment, as shown in Figs. S1 and S2a (online). Fig. S1b (online) illustrates the typical size of GO sheet applied as a typical precursor in this method. The surface and super depth images of single and secondary annealing GAF taken by a 3D microscopic system (KEYENCE, VHX-600E), as shown in Fig. 1b and Fig. S2c (online). Compared with the single annealing, the GAF surface obtained by the secondary annealing has less gullies and undulations on the surface, which proves that secondary annealing GAF is flatter, more regular, and denser. The X-ray diffraction (XRD) pattern of secondary annealed GAF (Fig. S2d, online) shows extremely sharp (002) peak at 26.59°, and a narrow full width at half maximum (FWHM) of 0.135° than single annealed of 0.235°, which proves that the secondary annealed GAF has higher crystallinity and interlayer regularity. In addition, the diffraction peak (004) indicates that GAF is highly graphitized. It has been proved that after the rolling and compressing process, structural defects are introduced into the single annealed GAF, which can be evidenced by the re-emerging D peak of the Raman spectrum (Fig. S2e, online). Such structural defects or lattice defects can be removed by the secondary annealing process [11]. In addition, the strong G peak at 1587 cm^{-1} demonstrates that GAF has highly sp^2 hybridized carbon atoms structure. All the characterization results prove that the secondary annealing treatment can improve the crystallinity and interlayer regularity of GAF, thus further enhance the electrical conductivity. The stress-strain curves of single annealing and secondary annealing GAF are tested, as shown in Fig. 1c. After the secondary annealing, the tensile strength of GAF is 59.78 MPa, which is an increase of 74.1% compared to the single annealing GAF (34.34 MPa). The longitudinal strain of the secondary annealing GAF is 3.81%, which is within the elastic range. The surface scanning electron microscope (SEM) image (Fig. S2f, online) shows that there are a lot of micro-wrinkles on the surface of GAF, which can provide cushioning force when the GAF is bent and improve the flexibility. The cross-section SEM image of GAF in Fig. S2g (online) demonstrates a GAF thickness of 15 μm. After secondary annealing and rolling compression, GAF becomes denser with the density of 1.92 g/cm^3. Compared with copper, GAF has higher thermal conductivity (1329 W/(m K)), as shown in the Fig. S2h (online). Furthermore, we

characterized the flexibility, mechanical stability, and chemical stability of GAF. As shown in Fig. S2i (online), after 20,000 times of fatigue resistance test, GAF maintains the original physical appearance, and its conductivity has not changed.

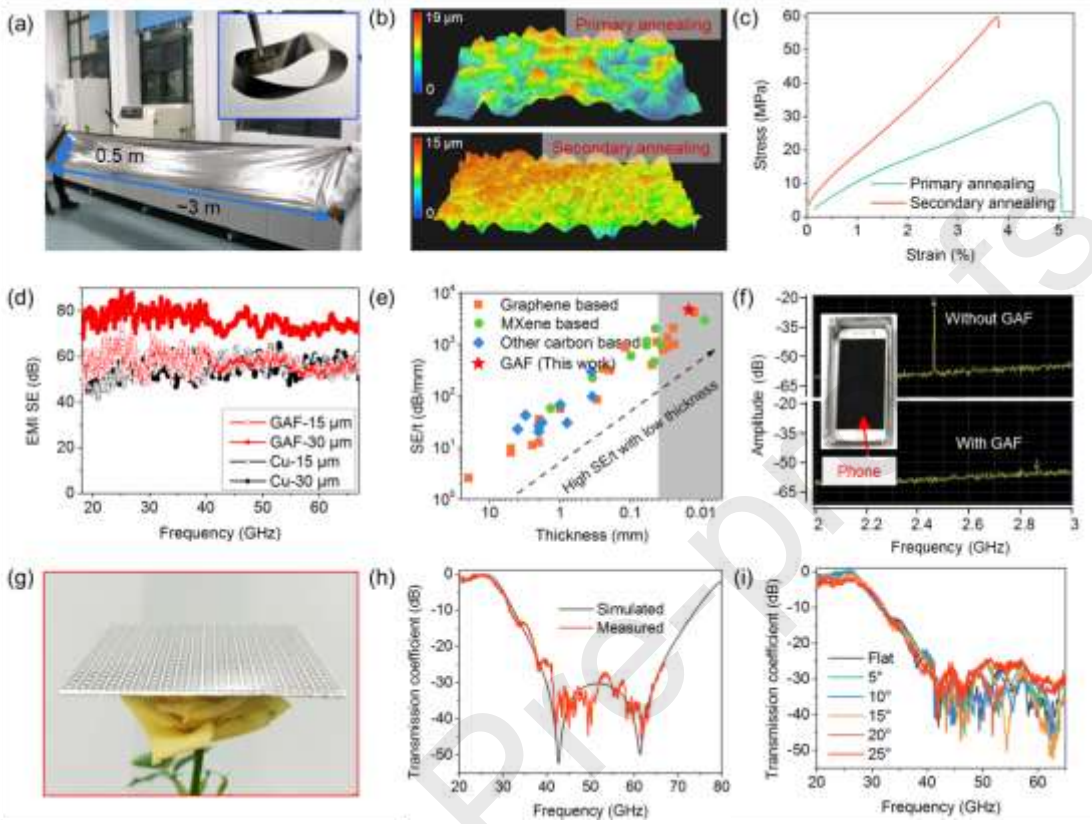

Fig. 1. (a) Digital photo of large format GAF with the size about 0.5 m × 3 m (illustration shows the high flexibility of the GAF). (b) The super depth images of single and secondary annealing GAF taken by a 3D microscopic system. (c) Stress-strain curves of single and secondary annealing GAF. (d) EMI SE of GAF with 15 and 30 μm among the frequency range of 2.6–67 GHz. (e) Comparison of SE/t in references with the result in this work. (f) The frequency spectrum of mobile phone RF signal in plastic box/GAF shielding box. (g) The digital photos of lightweight GAF FSS with 20×20 elements. (h) The simulated and measured transmission coefficient of double-layer GAF FSS in 20–80 GHz. (i) The transmission coefficient of GAF FSS in incident obliquely of electromagnetic wave.

The GAF has the advantages of light-weight, flexible, rapid heat conduction and easy to prepare in large scales, which is satisfied the requirement of modern electromagnetic protection materials. The electromagnetic interference shielding performance of GAF is test by the free space method. Fig. S3a (online) shows the

actual test environment of EMI SE. The vector network analyzer (Keysight PNA N5247A) is used to record the transmission coefficient and reflection coefficient of the standard gain horn antenna. According to the S-parameter, the EMI SE, reflectance, and transmittance of the test sample can be calculated. Fig. 1d clarifies the EMI SE of the GAF and copper foil between the frequency ranges of 18–67 GHz. The EMI SE of GAF with thickness of 15 μm is above 45–70 dB, which is similar to that of copper foil with the same thickness. When the thickness is increased to 30 μm, the EMI SE of copper foil remains unchanged, while the EMI SE of GAF is improved to 70–90 dB and higher than that of copper foil. In other words, the EMI shielding efficiency of GAF is as high as 99.99999% and 99.9999999% with the thickness of 15 and 30 μm, respectively. Thanks to the ultra-high conductivity, most of the energy of the electromagnetic wave is reflected on the surface of GAF and copper foil, and only small portion energy penetrates the surface into the interior of the EMI materials. Different from the isotropic structure of metal, GAF is a layered stacking structure with certain resistance. The electromagnetic wave energy entering the GAF can be repeatedly reflected and converted into thermal energy and then been absorbed. Therefore, the electromagnetic shielding performance of GAF will be improved with the increase of thickness. Based on the synergistic effect of reflection and absorption, the GAF has ultra-high electromagnetic shielding performance [13,14]. We compared the recently reported EMI shielding performance of graphene-based and other materials, as shown in Fig. S3b (online) GAF has the highest SE in the same thickness and the thinnest thickness in the same SE. Due to the importance of thickness to EMI shielding materials, EMI SE per unit thickness (SE/t) is used to characterize the EMI performance, as shown in Fig. 1e and Table S1 (online). At low frequency communication band (< 27 GHz), compared with other graphene-based structures, carbon nanotubes, carbon fibers and other materials, GAF has the highest SE/t (4666.67 dB/mm), which is comparable with MXene, and can be prepared in a large scale. For higher communication band, it is also the first time for two-dimensional materials-based macrostructure to be measured under millimeter wave (24–67 GHz).

To certify the practicability of GAF as EMI shielding material, we made an EMI shielding box by wrapping GAF on plastic box, as shown in Fig. S4a (online). Fig. S4b (online) illustrates the testing environment of EMI shielding box. The mobile phone which transmits radio frequency (RF) signal with a frequency of 2.45 GHz as the transmitter, and the horn antenna is connected to the spectrum analyzer as the

receiver. Fig. S4c (online) is the frequency spectrum of separately detecting the RF signal of the mobile phone and putting the mobile phone in the plastic box, which recorded by the spectrum analyzer (Agilent N9320B). The plastic box has no obvious attenuation for the RF signal. Fig. 1f shows the spectrum information of the transmitter placed in a plastic box with/without wrapped GAF. When the mobile phone is placed in a plastic box without wrapped GAF, the spectrum analyzer detects strong electromagnetic energy at 2.45 GHz. When the mobile phone is in EMI shielding box, the signal analyzer does not detect any signal, which elucidates that GAF has super strong EMI shielding performance. Video S1 (online) records the shielding effect of the box with GAF on mobile phone RF signals.

To further explore the electromagnetic protection of GAF, we designed a frequency selective surface (FSS) based GAF that works at millimeter wave frequency band, as shown in Fig. S5a and b (online). The square ring conductor layer and the dielectric layer, which compounded together by hot pressing [15], form the FSS of the double-layer structure. The GAF with a typical thickness of 15 μm is selected as the conductor of FSS. Polyethylene glycol terephthalate (PET) film (gray part) with a thickness of 0.06 mm, dielectric constant of 3.5 and loss tangent of 0.003 is the substrate of GAF FSS. The GAF FSS is produced by laser engraving method with the periodic element dimension of 3 mm×3 mm. Fig. S5c–e (online) show the design and optimization process, and the frequency response of different parameter values to GAF FSS. The inner diameter of the square ring and the size of the substrate have a severe influence on the operating frequency of the GAF FSS. The optimized parameter values are shown in Table S2 (online). Fig. S5f (online) illustrates the equivalent circuit diagram of GAF FSS element. The patch-type FSS periodic element is equivalent to a series circuit of resistance (R), inductance (L), and capacitance (C), where L and C represent the resonant frequency information, and R represents the Q value of the periodic element. The R, L, and C values are extracted by using optimization algorithm to adjust the circuit calculated results in Advanced Design System (ADS) software to match the EM simulated results of CST software. Fig. S5g (online) is the transmission coefficient results of the periodic element, which calculated the equivalent circuit by ADS software and simulated the actual model by CST software. The FSS resonates at 55 GHz with the –10 dB working frequency band of 43.10–66.20 GHz, and the calculated results are consistent with the simulation results. The E-field distribution can further analyze the working mechanism of FSS.

Fig. S5h and i (online) show the E-field distribution of the GAF FSS at operating frequency and non-operating frequency respectively. It can be clearly seen that there is no induced current in the FSS structure at non-operating frequency, and electromagnetic waves can pass through FSS normally. However, the FSS resonates at 55 GHz and generates a strong induced current, which causes electromagnetic waves cannot pass through the FSS.

To further broaden the working bandwidth, we designed a double-layer GAF FSS structure as shown in Fig. S6a (online). The interlayer spacing of GAF FSS is *d*, which is filled with a foam plate with a dielectric constant of 1.1. The foam plate with low dielectric constant has no affect electromagnetic waves of GAF FSS. Different interlayer spacing determines the performance of the double-layer GAF FSS. As the spacing decreases, the working bandwidth becomes wider. Increasing the spacing can enhance the rectangular coefficient and frequency selectivity of GAF FSS. Combining the two factors, we designed the layer spacing to be 1 mm, as show in Fig. S6b (online). After simulation optimization, GAF FSS is manufactured by laser engraving. We produced a GAF FSS with 20×20 periodic elements and the structure dimension of 60 mm×60 mm, as shown in Fig. 1g and Fig. S6c (online). GAF FSS has a very low areal density of 0.027 g/cm^2, demonstrating by that can be placed lightly on flowers. The measured and simulated transmission coefficient of GAF FSS under normal incidence of electromagnetic wave is shown in the Fig. 1h. In the 34.19–74.87 GHz frequency band, the transmission coefficient of GAF FSS is less than –10 dB, which means that FSS can shield more than 90% of the electromagnetic waves. GAF FSS can shield more than 99.9% of electromagnetic waves at frequency band of 42.71–66.75 GHz. Outside of this frequency band, electromagnetic waves can pass GAF FSS in a large proportion, proving that GAF FSS has good frequency selection characteristics. Fig. 1i depicts the spectrum curve of GAF FSS at different incident angles of electromagnetic waves. In the range of 0–25°, the transmission coefficient and working bandwidth of GAF FSS remain basically consistent. Fig. S6d (online) is the measurement environment and diagram of GAF FSS. GAF FSS is fixed on a rotatable wooden shelf and placed in microwave anechoic chamber to remove the influence of electromagnetic waves in the environment. The two horn antennas connected to the vector network analysis serve as the transmitter and receiver. The GAF FSS is placed vertically between the two horn antennas. The vector network analyzer (Keysight PNA N5247A) records the reflection coefficient and transmission

coefficient of the two antennas to calculate the frequency response of the GAF FSS. All the test results show that GAF is more suitable for modern electromagnetic protection materials with integrated thermal, light weight and high efficiency shielding.

In conclusion, the large-scale manufacture of an ultrahigh-conductivity graphene assembled film is achieved by secondary high temperature annealing. The conductivity of the treated GAF increases by 41% compared with the single annealing GAF and shows a high EMI SE of 70–90 dB and SE/t of 4666.67 dB/mm in frequency band of 18–67 GHz. In addition, a millimeter wave FSS based on GAF with 400 elements (3 mm × 3 mm) is designed and investigated for the first time. The GAF FSS has small areal density of 0.027 g/cm^2. In the 34.19–74.87 GHz frequency band, the transmission coefficient of GAF FSS is less than –10 dB, which means that FSS can shield more than 90% of electromagnetic waves. Within the frequency band of 42.71–66.75 GHz, GAF FSS can shield more than 99.9% of the electromagnetic waves. Moreover, inheriting the properties of GAF, the GAF FSS exhibits good flexibility, high thermal conductivity, and excellent mechanical stability. Thus, this research has demonstrated a new concept via applying a standard method that the graphene assembled films can be used in millimeter wave electromagnetic protection of EMI shielding and FSS, which can thus open a new research area.

Conflict of interest

The authors declare that they have no conflict of interest.

Acknowledgments

This work was supported by the National Natural Science Foundation of China (51701146 and 51672204), Wuhan Application Foundation Frontier Project (2020020601012220), and the Fundamental Research Funds for the Central Universities (WUT: 2020-YB-032, 205209016 and 2020IB005).

Author contributions

The manuscript was written through the contributions of all authors. Rongguo Song and Daping He had consideration for the idea and designed the experiments. Boyang Mao and Daping He oversaw the project progress. Rongguo Song, Shaoqiu Jiang,

Zelong Hu, Chi Fan, Peng Li, and Qi Ge performed the main experiments and analyzed the data. Rongguo Song, Boyang Mao, and Daping He wrote the manuscript.

References

[1] Cao MS, Wang XX, Zhang M, et al. Variable-temperature electron transport and dipole polarization turning flexible multifunctional microsensor beyond electrical and optical energy. Adv Mater 2020; 32: 1907156.

[2] Li W, Wei G, Pan X, et al. Electromagnetic compatibility prediction method under the multifrequency in-band interference environment. IEEE T Electromagn C 2018; 60: 520-528.

[3] Rathi V, Panwar V. Electromagnetic interference shielding analysis of conducting composites in near- and far-field region. IEEE T Electromagn C 2018; 60: 1795-1801.

[4] Cao M, Cai Y, He P, et al. 2D MXenes: electromagnetic property for microwave absorption and electromagnetic interference shielding. Chem Eng J 2019; 359: 1265-1302.

[5] Zhang M, Cao M, Shu J, et al. Electromagnetic absorber converting radiation for multifunction. Mater Sci Eng R 2021; 145: 100627.

[6] Song R, Chen X, Jiang S, et al. A graphene-assembled film based MIMO antenna array with high isolation for 5G wireless communication. Appl Sci 2021; 11: 2382.

[7] He P, Cao M, Cao W, et al. Developing MXenes from wireless communication to electromagnetic attenuation. Nano-Micro Lett 2021; 13:115.

[8] Iqbal A, Shahzad F, Hantanasirisakul K, et al. Anomalous absorption of electromagnetic waves by 2D transition metal carbonitride Ti_3CNT_x (MXene). Science 2020; 369: 446.

[9] Xing C, Zhu S, Ullah Z, et al. Ultralight and flexible graphene foam coated with Bacillus subtilis as a highly efficient electromagnetic interference shielding film. Appl Surf Sci 2019; 491: 616-623.

[10] Lai D, Chen X, Wang Y. Controllable fabrication of elastomeric and porous graphene films with superior foldable behavior and excellent electromagnetic interference shielding performance. Carbon 2020; 158: 728-737.

[11] Akbari A, Cunning BV, Joshi SR, et al. Highly ordered and dense thermally conductive graphitic films from a graphene oxide/reduced graphene oxide mixture. Matter 2020; 2: 1198-1206.

[12] Song R, Wang Q, Mao B, et al. Flexible graphite films with high conductivity for radio-frequency antennas. Carbon 2018; 130: 164-169.

[13] Wen B, Cao M, Lu M, et al. Reduced graphene oxides: light-weight and high-efficiency electromagnetic interference shielding at elevated temperatures. Adv Mater 2014; 26: 3484-3489.

[14] Cao M, Song W, Hou Z, et al. The effects of temperature and frequency on the dielectric properties, electromagnetic interference shielding and microwave-absorption of short carbon fiber/silica composites. Carbon 2010; 48: 788-796.

[15] Song R, Zhao X, Wang Z, et al. Sandwiched graphene clad laminate: a binder-free flexible printed circuit board for 5G antenna application. Adv Eng Mater 2020; 22: 2000451.

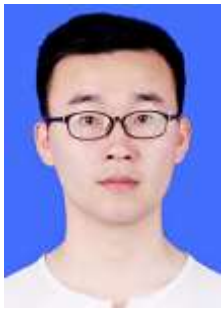

Rongguo Song received his Ph.D. degree from Hubei Engineering Research Center of RF-Microwave Technology and Application, Wuhan University of Technology (WUT) in 2021. His research interest includes graphene based materails, RF and microwave devices design.

Boyang Mao is a Hughes Hall research associate at the University of Cambridge. He obtained his Ph.D. degree in Chemistry from the University of Bath. He became a postdoctoral fellow at the National Graphene Institute, University of Manchester and then moved to the Cambridge Graphene Centre. His research interest includes the preparation and application of graphene and related two-dimensional materials in environmental science, sustainable technologies, and flexible electronics.

Daping He is a full professor at WUT. He obtained his Ph.D. degree in Materials Processing Engineering from WUT in 2013. He was a postdoctoral fellow at University of Science and Technology of China. Then he joined University of Bath as a Newton International Fellow and University of Cambridge as a postdoctoral fellow. His research interest is preparation and application of nanocomposite materials into new energy devices, sensors and RF microwaves field.

Graphic Abstract

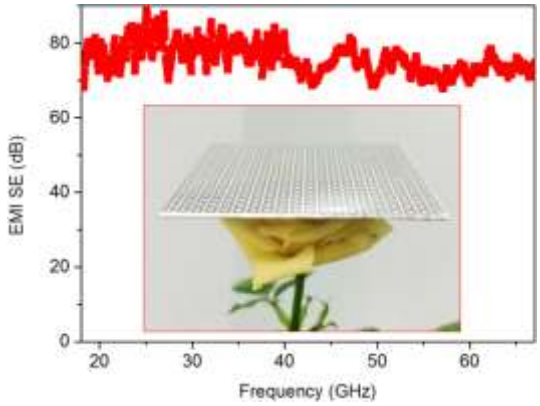

In this work, we proposed a large-scale graphene assembled film with ultra-high conductivity for millimeter wave electromagnetic protection. The electromagnetic interference shielding and frequency selective surface based on graphene assembled film show excellent performance.